

FUNCTIONALIZED CELLULOSE BEADS WITH ACTIVATED CARBON Fe₃O₄/CoFe₂O₄ FOR CATIONIC DYE REMOVAL

SEYEDEHMARYAM MOOSAVI,* SINYEE GAN** and SARANI ZAKARIA***

**Nanotechnology and Catalysis Research Centre (Nanocat), Institute of Postgraduate Studies (IPS),
University of Malaya, 50603 Kuala Lumpur, Malaysia*

***Information Technology and Corporate Services Division, Malaysian Palm Oil Board,
6, Persiaran Institusi Bandar Baru Bangi, 43000 Kajang, Selangor, Malaysia*

****Bioresources and Biorefinery Laboratory, Faculty of Science and Technology,
Universiti Kebangsaan Malaysia, 43600 UKM Bangi, Selangor, Malaysia*

✉ *Corresponding authors: Sinyee Gan, gansinyee@hotmail.com*

Sarani Zakaria, szakaria@ukm.edu.my

Received September 21, 2018

Modified regenerated cellulose beads functionalized with activated carbon (AC), as well as magnetic cellulose beads of AC-Fe₃O₄ and AC-CoFe₂O₄, were synthesized. The AC was further used as adsorbent for the removal of cationic methylene blue (MB) dye from aqueous solution. The magnetic cellulose beads possessed a high magnetic response to an external magnetic field and their ease of recovery could be facilitated with the aid of a magnetic field. The synthesized adsorbents were characterized using a Field Emission Scanning Electron Microscope (FESEM), as well as by energy dispersive X-ray (EDX) spectrometry and thermogravimetric analysis (TGA). In comparison with the synthesized magnetic cellulose beads, the maximum adsorption capacity of the adsorbent beads assisted with AC, AC-Fe₃O₄ and AC-CoFe₂O₄ was of 54, 53 and 50 mg/g, respectively. The kinetic study of the adsorption of MB dye onto the adsorbents was performed at different parameters (initial dye concentration and temperature). The kinetics of the adsorption fit well with the pseudo-second-order model.

Keywords: adsorbent recovery, biomass, kinetic, magnetite, separation

INTRODUCTION

The treatment of wastewaters coming from industrial activities is a topical issue in biological and environmental science and technology, as wastewaters represent a major cause of degradation of water quality. Dyes originating from a wide variety of industrial sources are stable and resistant to biodegradation because of their complex aromatic molecular structure. They are the main sources of environmental pollution.¹ The adsorption-based technology is one of the established techniques for addressing the removal of both local and global environmental contaminants.^{2,3} Physical adsorption can be a trusty alternative due to its advantages in terms of the infrastructure cost, modular design, simplified technological design, operation and the wide availability of the adsorbents.^{4,5} This method is very dependent upon the type of the adsorbent used (*e.g.* activated carbon (AC), biomass, polymer, nanomaterial *etc.*).⁶ The cost of

adsorbent production is not the only factor involved in developing an excellent adsorbent. The adsorption performance, regeneration ability and adsorbent separation are other important features of an effective adsorbent.⁷

Much research has been carried out on the use of biodegradable polymers with high adsorption capacities. The use of highly abundant low-cost renewable bioresources allows the development of products with a low impact on the environment.^{8,9} Cellulose, a relatively stable polymer with high axial stiffness and high crystallinity, is considered to be the most common renewable polysaccharide on earth.^{10,11} The presence of numerous hydroxyl groups gives a cationic nature to the biopolymer and helps cellulose, as a bioaffinity carrier material, to improve the adsorption capability.¹² In recent years, cellulose-based materials have been frequently used in water treatment studies as a

biocompatible adsorbent. However, because of its low adsorption capacity, an interesting area of research focusing new cellulose-based composite adsorbents with high adsorption capacity has been developed.

A magnetic adsorbent is considered to be an effective and rapid adsorption separation technique due to its better separation capability and lower energy requirement.^{13,14} So far, one of the most promising ways for a novel environmental purification method is magnetic separation due to its capability of treating a large amount of wastewater within a short period of time, without producing contaminants, such as flocculants.¹⁵ One of the disadvantages of cellulose-based adsorbents is the difficulty to separate them and recover. Magnetic separation is a promising strategy to promote easy and fast recovery for valuable adsorbents and further reuse.¹⁶ Currently, Fe_3O_4 is widely studied in separation technology researches due to its excellent chemical stability, simple surface modification, cost-effective preparation, high surface area and biocompatibility, which is highly suitable in the adsorption technology for environmental protection.¹⁷ In addition, CoFe_2O_4 shows an interesting magnetic property among ferrites, which is attributed to its excellent chemical stability, moderate saturation magnetization and mechanical hardness.

The employment of magnetic adsorbents could enhance the thermal stability and the cross-linking density of the adsorbents.^{18,19} Coating Fe_3O_4 and CoFe_2O_4 with cellulose could enhance the stability of dispersed nanoparticles by preventing their aggregation and oxidation.²⁰ AC is one of the most widely studied and promising adsorbents for environmental pollution control due to its high surface area and high adsorption capability to remove a large number of organic compounds.²¹ Among other low-cost agricultural wastes, coconut shell AC has a very high dye removal capability due to the presence of some functional groups, such as carboxylic, hydroxyl and lactone.²² So, the fabrication of new promising adsorbents using a combination of carbon materials with magnetic Fe_3O_4 and CoFe_2O_4 particles will give some advantages. By comparing the adsorption capability of these adsorbents, we can explore more possibilities for obtaining an adsorbent with high adsorption capacity and with ease of recovery using a magnetic field.

In this study, a green method was used for preparing cellulose biopolymer beads as supporting materials and for the functionalization of AC with $\text{Fe}_3\text{O}_4/\text{CoFe}_2\text{O}_4$ composite, with the objective of developing an efficient adsorbent for dye removal from water. The combination of AC and magnetic materials with cellulose was carried out to obtain novel composite adsorbents for the removal of hazardous materials, such as dyes, from water bodies, and their adsorption behaviours were compared. In this paper, the structure and the adsorption behaviors of the magnetic cellulose-based beads (MCB) for the removal of methylene blue (MB) were examined and the adsorption equilibrium was evaluated. The effects of solution pH, initial MB concentration and temperature on MB removal, as well as kinetics, were also investigated to evaluate the desirability of the developed adsorbents for application in the water treatment field.

EXPERIMENTAL

Materials

Raw kenaf core was supplied by the Malaysian Agricultural Research and Development Institute (MARDI). Coconut shell activated carbon (AC) powder (200 mesh) was purchased from Bravo Green Sdn. Bhd. (Sarawak, Malaysia). Sodium hydroxide (NaOH) and urea were obtained from R&M Chemicals. Fe_3O_4 and 98.8% sulfuric acid were purchased from Sigma Aldrich. All the chemicals were used without further purification. Stock solutions of methylene blue (MB) trihydrate (Sigma Aldrich) were prepared by dissolving 1 g MB powder in 1 L distilled water. Standard calibration of diluted MB solutions was performed using a UV-Vis spectrophotometer (Jenway 7315 Spectrophotometer) at a λ_{max} of 664 nm. Different initial concentrations of MB dye solutions were obtained by diluting the stock solution in accurate proportions.

The raw kenaf core was soda pulped in a digester with 25% NaOH concentration at 170 °C for 150 min. The kenaf core pulp (KCP) was bleached using a four-stage bleaching method (DEED), as described in previous literature.²³ Stage D consisted in a treatment with 1.7% NaClO_2 for 4 h at 80 °C. Stage E was an alkaline treatment on KCP with 4-6% NaOH solution for 3 h at 80 °C. The cellulose was rinsed after every single stage to remove the bleaching chemicals. Proper rinsing was important for removing lignin from the sample, prior to the next stage. The bleached kenaf core cellulose was then dried for 24 h at 105 °C.

Preparation of CoFe_2O_4 nanocrystals

CoFe_2O_4 nanocrystals were synthesized by reacting $\text{CoCl}_2 \cdot 6\text{H}_2\text{O}$ with a $\text{FeSO}_4 \cdot 7\text{H}_2\text{O}$ solution, using the

simple hydrothermal method, as it was reported in our previous study.²⁴

Preparation of magnetic cellulose beads

Optimal extrusion dropping technology was used for the fabrication of cellulose beads. 3 g of bleached kenaf core cellulose was dissolved in 100 g mixed solutions of NaOH/urea/distilled water at the ratio of 7:12:81 at -13 °C, under vigorous mechanical stirring, to form a transparent cellulose solution. Then, 12 wt% of AC was added into the cellulose solution and mixed homogeneously to form AC cellulose beads, while magnetic cellulose beads were produced by modifying AC with 5 wt% of each Fe₃O₄ and CoFe₂O₄. The formation of homogeneous spherical modified cellulose beads was performed by adding dropwise the mixture of cellulose solution using a syringe pump into a coagulation bath of sulfuric acid (250 mL, 10 wt%) at 20 °C. The prepared cellulose beads were washed several times to remove excess of acidic coagulation and were kept in distilled water for further use.

Characterization

The morphology of the prepared beads was observed with a field emission scanning electron microscope (FESEM), and the elemental concentration was measured by energy dispersive X-ray (EDX) spectroscopy. Thermogravimetric analysis (TGA) was performed to study the thermal properties of freeze-dried beads as a function of increasing temperature (from room temperature to 600 °C at a constant heating rate of 10 °C/min).

Adsorption

Different initial concentrations of MB dye solutions (500, 400, 300, 200 and 100 mg/L) were prepared by diluting the stock solution in accurate proportions. A standard calibration of diluted MB solutions was measured using a UV-Vis spectrophotometer (Jenway 7315 Spectrophotometer) at a λ_{max} of 664 nm. The pH of the MB dye solution was adjusted by adding hydrochloric acid and NaOH solution. The pH was measured using a pH meter (Eutech pH Tester10). A calibration curve, which fitted the Beer-Lambert law, was generated for the adsorbate solutions using a series of dilutions ranging from 0.01 to 1 mM dye solutions.

In order to study the effect of initial dye concentration on the adsorption capacity and removal percentage, the adsorbents (AC cellulose beads, AC-CoFe₂O₄ and AC-Fe₃O₄ cellulose beads were standardized as 1 gram of dry beads) were added into a beaker. The beaker contained 100 mL fixed concentration of MB solution, with different initial dye concentrations (500, 400, 300, 200 and 100 mg/L), at fixed pH 7 and 20 °C. The effect of temperature was studied at 20 °C, 40 °C and 60 °C, pH 7 and an initial dye concentration of 200 mg/L was fixed. The mixture was stirred with a magnetic stirrer at 250 rpm until it reached the adsorption equilibrium. Aliquots of the

solution (200 μ L) were withdrawn at various intervals of time and were added to distilled water (in a ratio of 1:19) in polystyrene 4 mL cuvettes. The concentration of MB was determined using a UV-Vis spectrophotometer.

RESULTS AND DISCUSSION

Characterization of the prepared cellulose magnetic beads

FESEM images of native cellulose beads, AC cellulose beads and magnetic beads are exhibited in Figure 1. The surface of the adsorbents presented macro- to nanoporous structures. However, the porous structure was slightly diminished after AC was embedded, which was due to the hydrogen bond between cellulose and AC.²⁵ Morphological micrographs of embedded AC cellulose beads showed almost similar structure to that of the beads functionalized with each Fe₃O₄ and CoFe₂O₄ particles. This indicated that the presence of magnetic particles on the AC and cellulose beads did not significantly affect the porous structure of the cellulose beads.^{26,27}

The EDX analysis and spectra of AC cellulose beads, AC-CoFe₂O₄ and AC-Fe₃O₄ cellulose beads (c) are shown in Figure 2. From this figure, it can be detected that the AC-Fe₃O₄ cellulose beads consisted of mainly 67.2% C (carbon), 31.1% O (oxygen) and 1.7% Fe (iron), while the AC-CoFe₂O₄ cellulose beads consisted of 74.6% C, 23.5% O, 1.4% Fe and 0.5% Co (cobalt).

Figure 3 shows the TGA curves of the AC cellulose beads and magnetic cellulose beads measured in the temperature range of 29 to 600 °C. It reveals that the weight loss of the AC cellulose beads and AC-Fe₃O₄ cellulose beads occurred in three stages. The first stage occurred at temperatures below 100 °C and represented an about 9% weight loss. This could be the consequence of removing the adsorbed water and residue of acetic acid.²⁸ The second and third regions, which ranged at 150-220 °C and 250-450 °C, represented weight losses of about 4% and 14%, respectively. This indicated the decomposition of the beads and the degradation of the remaining polymer chains.²⁹ The TGA curve of the AC-CoFe₂O₄ cellulose beads showed two regions of weight loss. The first region was due to the adsorbed water. The second region, at 120-450 °C, represented a weight loss of about 14%. The weight loss of magnetic cellulose beads in the last degradation stage can be explained by the fact that the decomposition of polymer would produce reducing gas, which might react with Fe₃O₄.¹⁸

Figure 3 illustrates that the addition of CoFe_2O_4 and Fe_3O_4 into the AC cellulose beads has enhanced the thermal stability of the adsorbents. The reason could be that, as metal particles remained within the polymer networks, they could incorporate some polymer chains in

their crystalline lattice, thereby delaying the degradation process.³⁰ Moreover, this figure shows that the residual weight below 450 °C increased with the addition of magnetite and the prepared magnetic cellulose beads possessed high thermal stability.

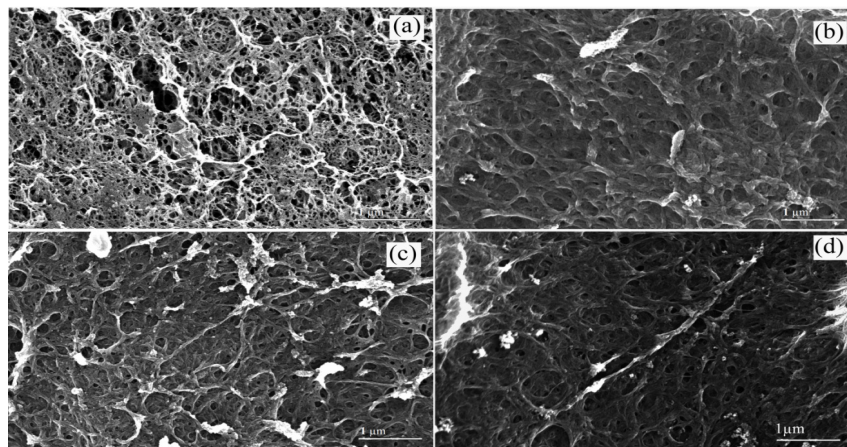


Figure 1: Micrographs of (a) cellulose beads, (b) AC cellulose beads, (c) AC- CoFe_2O_4 cellulose beads and (d) AC- Fe_3O_4 cellulose beads

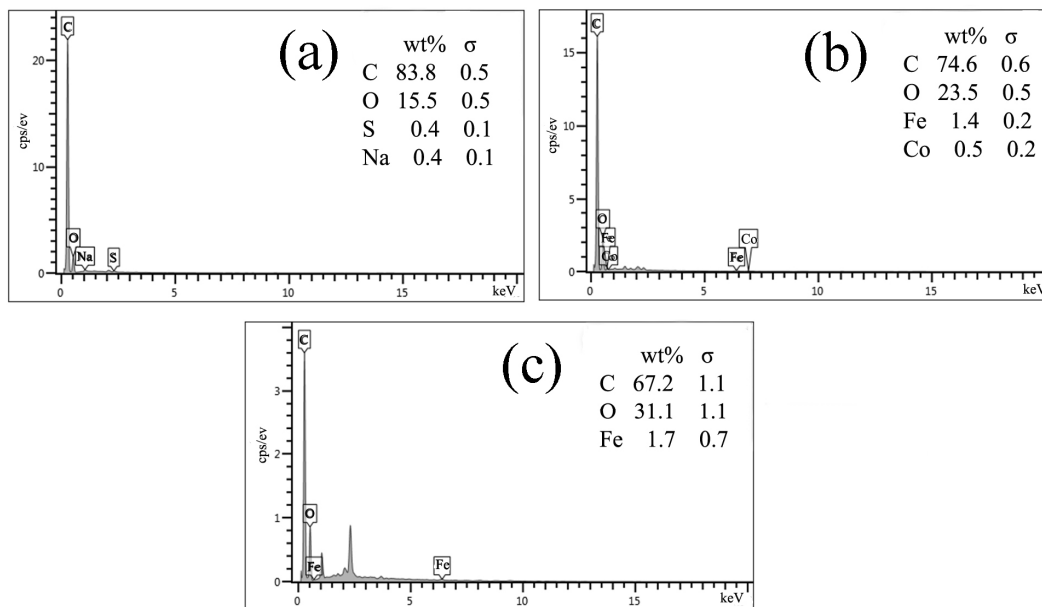


Figure 2: EDX analysis results of (a) AC cellulose beads, (b) AC- CoFe_2O_4 cellulose beads and (c) AC- Fe_3O_4 cellulose beads

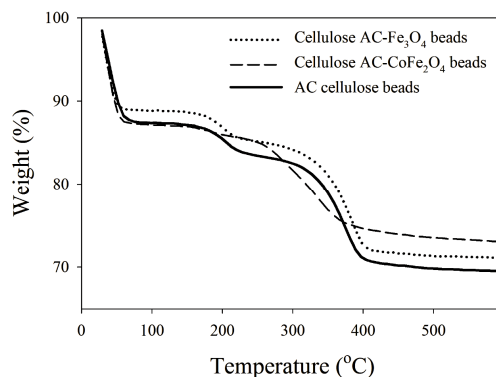


Figure 3: TGA curves of AC cellulose beads and magnetic cellulose beads

Kinetic studies on MB dye adsorption

The preliminary adsorption kinetic analysis of AC functionalized cellulose beads assisted by each CoFe_2O_4 and Fe_3O_4 is observed in Figure 4 (a). From the observation, the neat cellulose beads show a very low MB uptake, as it achieved the adsorption equilibrium in 20 minutes. The MB uptake kinetics towards AC occurred in a rapid reaction and achieved the adsorption equilibrium in less than 10 minutes. Meanwhile, the MB uptake of AC functionalized cellulose beads was improved significantly with the aid of AC, although the AC embedded in the regenerated cellulose system hindered the MB uptake, and achieved complete adsorption after 90 minutes. Moreover, the adsorption capacity of AC and functionalized cellulose beads showed an insignificant difference, explained by the slight change of the overall structure after the modification. Additionally, due to the presence of magnetic particles on the cellulose beads, the AC- CoFe_2O_4 and AC- Fe_3O_4 cellulose beads possessed high affinity for magnetic separation using an external magnetic field and could be easily recovered after water remediation (see Fig. 4 (b)). The introduction of the AC filler with excellent adsorption properties into the cellulose beads was aimed to improve the adsorption equilibrium of the cellulose. This has proven the feasibility of the developed advanced adsorbents in the treatment process, revealing their potential to be utilized in a real application in the future.

The effect of pH was investigated in the range of pH 3-9, at a fixed initial concentration of 200 mg/L at 20 °C. There was a slightly distinctive uptake of MB onto the AC cellulose beads at the series of pH 3, 5, 7, and 9 of 19.77, 20.57, 21.27 and 21.21 mg/g, respectively. It could be confirmed that the adsorption was mainly due to

the contribution of the encapsulated AC, as it was not pH-sensitive. The AC played an important role in the improvement of the adsorption capacity.³¹ Therefore, as reported earlier, pH 7 was selected as the optimum medium.⁷

The mechanism of adsorption on the surface of the adsorbent beads was investigated using several kinetic models. Pseudo-first-order, pseudo-second-order and intraparticle diffusion equations were used to find the best-fitted model. For the pseudo-first-order model, it was assumed that the change of solute uptake was directly proportional to the difference in saturation concentration. The amount of solid uptake could be defined as in Equation 1:

$$\log(q_e - q_t) = \log q_e - \frac{k_1 t}{2.303} \quad (1)$$

where k_1 (min^{-1}) is the pseudo-first-order rate constant and q_e and q_t are the adsorption capacity (mg g^{-1}) of MB onto the magnetic beads at equilibrium and at time t (min), respectively.

The pseudo-second-order model explained the rate dependence on the capacity of adsorption in the solid phase, but no dependence on the concentration of the adsorbed substance was found. It is given in Equation 2:³²

$$\frac{t}{q_t} = \frac{1}{k_2 q_e^2} + \frac{t}{q_e} \quad (2)$$

where k_2 ($\text{g mg}^{-1} \text{min}^{-1}$) is the pseudo-second-order rate constant of adsorption. The correlation coefficients (R^2) and kinetic parameters were obtained by non-linear plots, as shown in Figure 5 and summarized in Table 1. The results showed the correlation coefficients' (R^2) values of the pseudo-second-order model were higher than 0.992 for all the three types of adsorbent. The adsorption capacities calculated by the model (q_{cal}) were closer to experimental adsorption

capacities (q_e exp). Therefore, the pseudo-second-order model could better be fitted and described

best the adsorption process of MB dye onto the AC cellulose beads and magnetic cellulose beads

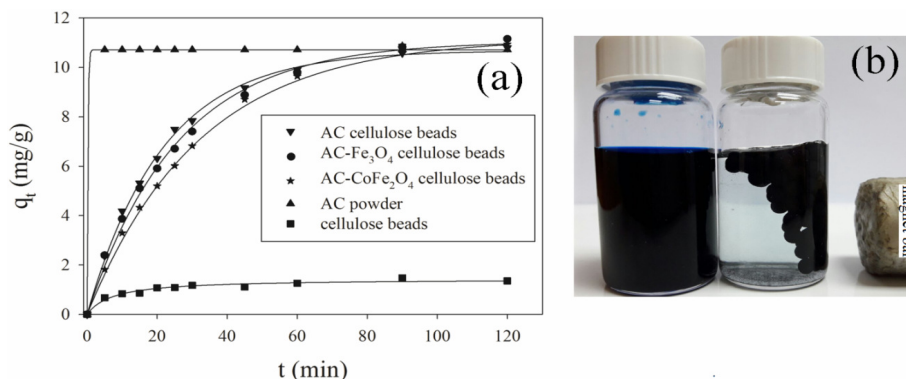


Figure 4: Preliminary analysis of (a) adsorption kinetics onto AC cellulose beads, AC-Fe₃O₄ cellulose beads, AC-CoFe₂O₄ cellulose beads and AC powder in 100 mg/L MB dye concentration, and (b) magnetic separation of magnetic cellulose beads from the solution by an external magnetic field

The adsorption proceeded in three main steps, including instantaneous surface adsorption, intraparticle diffusion, and final equilibrium. In most adsorption processes, the adsorption capacity varies almost proportionally with $t^{1/2}$ rather than with t . This model is called intraparticle diffusion and can be expressed as:

$$q_t = k_i t^{\frac{1}{2}} \quad (3)$$

where q_t is the adsorption capacity at time t , and k_i (mg/g min^{1/2}) is the intraparticle diffusion constant rate, which can be determined from the slope of the linear plot of q_t versus $t^{1/2}$.

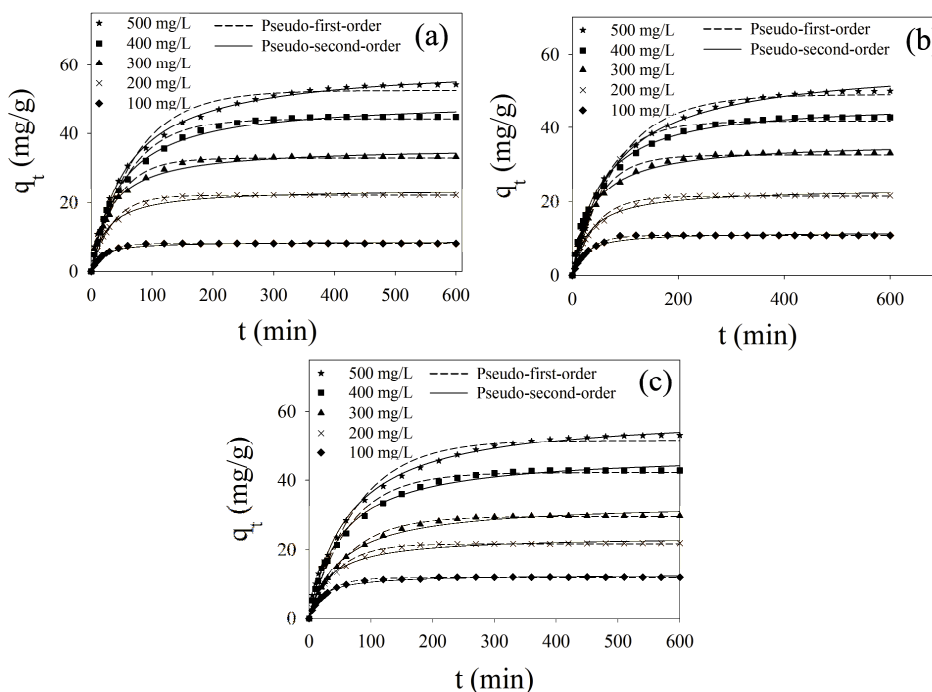


Figure 5: Pseudo-first-order and pseudo-second-order plots of MB adsorption kinetics onto: (a) AC cellulose beads, (b) AC-CoFe₂O₄ and (c) AC-Fe₃O₄ cellulose beads (initial concentration)

Table 1
Pseudo-first-order, pseudo-second-order and intraparticle diffusion parameters for adsorption of MB dye

Adsorbents	Initial dye concentration (mg/L)	Pseudo-first-order				Pseudo-second-order				Intraparticle diffusion	
		q_e exp (mg/g)	q_e cal (mg/g)	K_1 (1/min)	R^2	q_e exp (mg/g)	q_e cal (mg/g)	K_1 (1/min)	R^2	K_1 (mg/g min ^{1/2})	R^2
AC cellulose beads	100	8.309	8.3068	0.0185	0.9990	8.309	9.6682	0.0052	0.9926	0.63	0.861
	200	22.244	21.9261	0.0129	0.9939	22.244	25.7478	0.0013	0.9975	1.476	0.9108
	300	33.343	32.5090	0.0108	0.9869	33.343	37.4816	0.0008	0.9950	1.816	0.909
	400	44.9	43.6509	0.0076	0.9899	44.9	51.5429	0.0004	0.9985	2.369	0.935
	500	54.236	52.5399	0.0061	0.9852	54.236	60.3293	0.0003	0.9977	2.211	0.9123
AC-Fe ₃ O ₄ cellulose beads	100	11.281	11.1821	0.0164	0.9963	11.281	13.1833	0.0033	0.9969	0.8657	0.9015
	200	21.727	21.3857	0.0103	0.9919	21.727	25.4617	0.0010	0.9980	1.3864	0.9367
	300	35.1617	29.3548	0.0070	0.9967	35.1617	29.713	0.0005	0.9984	1.6221	0.9343
	400	42.781	41.5122	0.0071	0.9878	42.781	49.3896	0.0004	0.9978	2.2612	0.9495
	500	53.202	51.6592	0.0056	0.9861	53.202	59.7452	0.0003	0.9977	2.1987	0.923
AC-CoFe ₂ O ₄ cellulose beads	100	10.96	11.0899	0.0138	0.9946	10.96	13.4272	0.0025	0.9935	0.8851	0.919
	200	21.62	21.1289	0.0104	0.9889	21.62	25.0957	0.0011	0.9980	1.3671	0.9398
	300	33.156	32.1726	0.0093	0.9859	33.156	37.0206	0.0007	0.9973	1.6626	0.9152
	400	42.839	41.1581	0.0073	0.9794	42.839	47.7224	0.0004	0.9956	2.0204	0.9354
	500	49.93	48.9675	0.0050	0.9946	49.93	57.6746	0.0002	0.9980	2.1746	0.9171

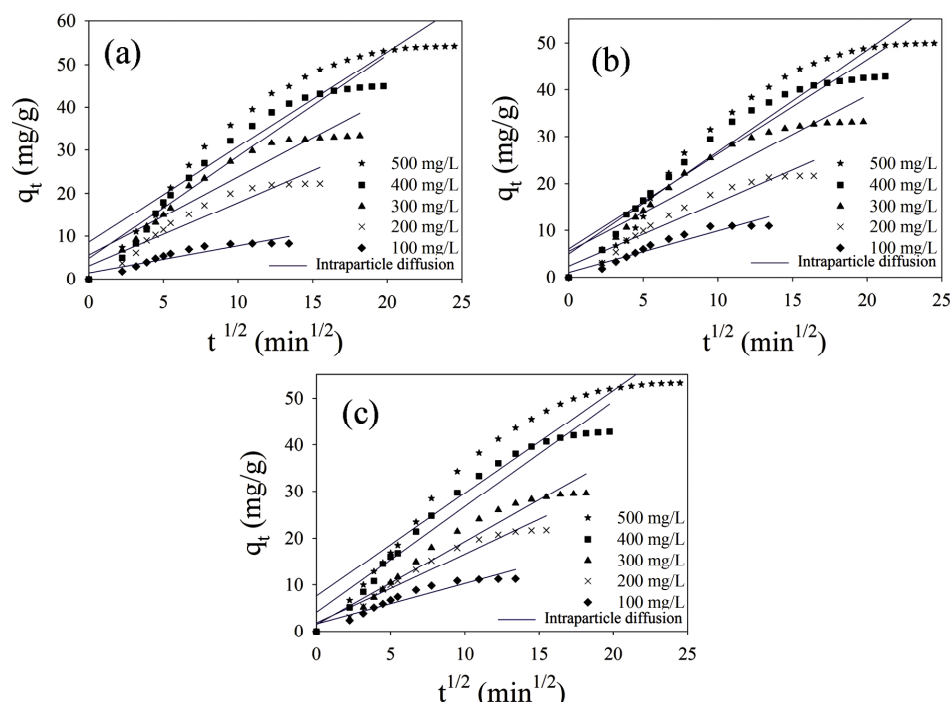


Figure 6: Intraparticle diffusion adsorption of MB onto: (a) AC cellulose beads, (b) AC-CoFe₂O₄ and (c) AC-Fe₃O₄ cellulose beads at a different initial concentration

Figure 6 shows the intraparticle diffusion kinetics of MB dye adsorption onto the AC cellulose beads. From this figure, the three main steps of the intraparticle diffusion model, with different rates, could be observed. The adsorption of MB dye at 100 mg/L dye concentration showed multi-linearity and indicated that the adsorption of MB involved two or more steps.³³ At higher concentrations, the plots tended to represent one slope. This could be due to the simultaneous occurrence of surface adsorption and intraparticle diffusion.³⁴

Effect of initial dye concentration

Figure 5 shows the effect of contact time on the adsorption capacity of MB onto the AC cellulose beads and magnetic cellulose beads at different initial concentrations. It was demonstrated that the adsorption capacity of 100 mg/L of MB dye rapidly increased at the initial adsorption stage, then continued to increase with contact time at a relatively slow rate. As mentioned before, the presence of AC

with its high adsorption capacity and large surface area, as well as the existence of abundant -OH groups in the magnetic cellulose beads, leads to a high adsorption potential in aqueous dye solutions. The results showed that at the beginning, the dye was adsorbed onto the exterior surface of the adsorbent beads, which increased the adsorption rate. Then, the exterior surface became saturated, and the dyes needed to penetrate into the bead pores to be adsorbed onto the inner surface of the adsorbent. The adsorption process at different initial MB dye concentrations reached the equilibrium level within 90-390 min and there was no significant difference after the equilibrium was achieved. It indicated that the equilibrium time was an important parameter in water treatment applications. As shown in Figure 5, the MB adsorption capacity increased with increasing initial dye concentrations, due to a significant driving force to overcome the mass transfer resistance of the dye molecules between the solid phase adsorbent and the liquid phases.

Moreover, results showed that the adsorption capacity of the AC cellulose beads was almost similar to that of the AC-Fe₃O₄ cellulose beads and slightly higher than that of the AC-CoFe₂O₄ cellulose beads, which can be attributed to the surface area and pore size.²⁶ The presence of CoFe₂O₄ in the AC beads leads to a decrease in the surface area and total pore volume, as the CoFe₂O₄ has a lower

surface area that covers the AC surface more than Fe₃O₄.^{26,27} It should be mentioned that the slight difference in the adsorption capacity of the AC-CoFe₂O₄ beads, as compared to the AC cellulose beads, was most probably due to the independent effect of the presence of CoFe₂O₄ on the pore volume of AC (as illustrated in Fig. 1).

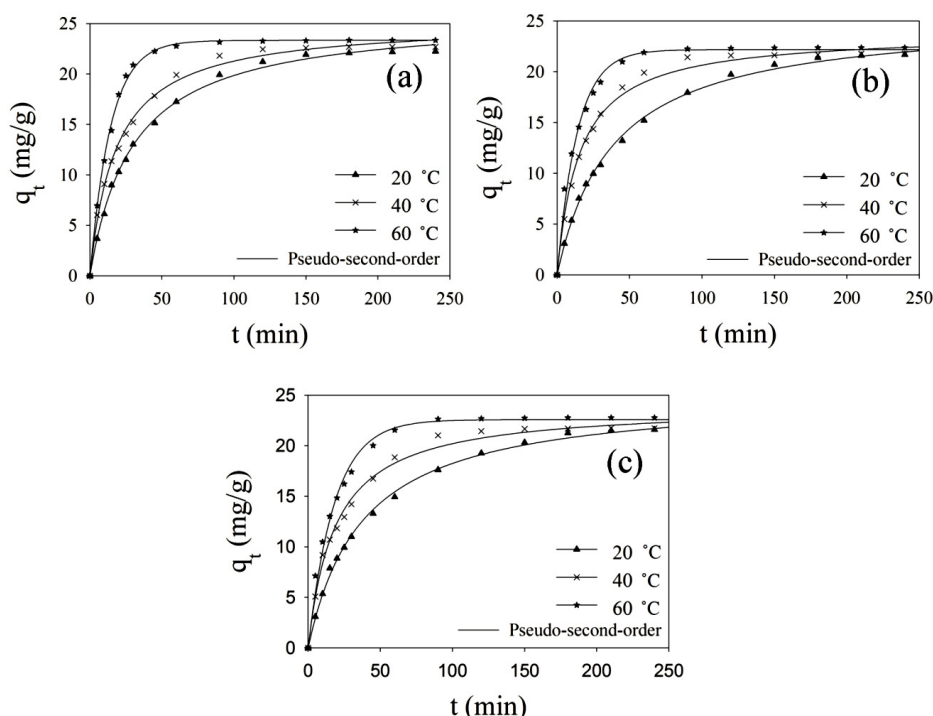


Figure 7: Effect of temperature on the adsorption capacity of (a) AC cellulose beads, (b) AC-CoFe₂O₄ and (c) AC-Fe₃O₄ cellulose beads towards MB dye

Effect of temperature

Temperature is considered as another significant parameter that can affect the adsorption process of dyes. Figure 7 shows the effect of temperature on the adsorption of MB dye onto the AC cellulose beads and magnetic cellulose beads at pH 7 and the initial dye concentration of 200 mg/L at the temperatures of 20 °C, 40 °C and 60 °C. Temperature can affect the dyes mobility and solubility.³⁵ If increasing temperature causes an increase in the adsorption capacity, the adsorption process is meant as an endothermic process.³⁶ As shown in Figure 7, increasing the temperature caused an increase in the adsorption capacity and the transfer of the adsorbate species towards the interior of the adsorbent. This could be due to the increase in the mobility of

the dye molecules and the increase in the number of active sites for the adsorption.

Moreover, this adsorption improvement could be due to the chemical interaction between the adsorbent and the adsorbate, considering the construction of some new adsorption sites. The amplified rate of intraparticle diffusion of the adsorbate species into the activated adsorbent pores could be another reason for improved adsorption.³⁷⁻⁴⁰ Therefore, the adsorption of MB dye onto the AC cellulose beads and magnetic cellulose beads is confirmed as an endothermic process. Economically, the contact time to reach the equilibrium point is considered an important parameter. The resultant data show that the equilibrium times of adsorption at 20, 40 and 60 °C were about 120, 90 and 60 min, respectively.

CONCLUSION

Embedding AC and/or magnetic particles into cellulose beads was performed successfully and cationic MB dye was adsorbed effectively onto AC cellulose beads and magnetic cellulose beads. FESEM images revealed that the presence of magnetic particles did not significantly affect the porosity of the cellulose beads. TGA results indicated that the prepared cellulose beads had excellent thermal stability. The thermal stability of the AC cellulose beads has been enhanced with the aid of CoFe₂O₄ and Fe₃O₄. The adsorption efficiency of the AC cellulose beads was almost similar to that of the AC-Fe₃O₄ cellulose beads, but slightly higher than that of the AC-CoFe₂O₄ cellulose beads. The adsorption process was best described by the pseudo-second-order model. The magnetic sensitivity of the magnetic cellulose beads under an external magnetic field provides an easy way for separating MB from water. The developed magnetic cellulose beads could be used as effective and promising adsorbents for the removal of MB dye, as the AC is expensive, while the adsorption efficiency of neat cellulose is not sufficient.

ACKNOWLEDGEMENT: The authors thank the Universiti Kebangsaan Malaysia for the financial support *via* the research project grant DIP-2018-033. The authors are also thankful to the Centre for Research and Instrumentation Management (CRIM) at UKM for providing the testing services.

REFERENCES

- ¹ K. B. Tan, M. Vakili, B. A. Horri, P. E. Poh, A. Z. Abdullah *et al.*, *Sep. Purif. Technol.*, **150**, 229 (2015), <https://doi.org/10.1016/j.seppur.2015.07.009>
- ² G. Li, Y. Li, Z. Wang and H. Liu, *Mater. Chem. Phys.*, **187**, 133 (2017), <https://doi.org/10.1016/j.matchemphys.2016.11.057>
- ³ R. Uma, K. Ravichandran, S. Sriram and B. Sakthivel, *Mater. Chem. Phys.*, **201**, 147 (2017), <https://doi.org/10.1016/j.matchemphys.2017.08.015>
- ⁴ M. Elkady, A. M. Ibrahim and M. A. El-Latif, *Desalination*, **278**, 412 (2011), <https://doi.org/10.1016/j.desal.2011.05.063>
- ⁵ S. Kittappa, S. Pichiah, J. R. Kim, Y. Yoon, S. A. Snyder *et al.*, *Sep. Purif. Technol.*, **153**, 67 (2015), <https://doi.org/10.1016/j.seppur.2015.08.019>
- ⁶ L. Ai, M. Li and L. Li, *J. Chem. Eng. Data*, **56**, 3475 (2011), <https://doi.org/10.1021/je200536h>
- ⁷ M. S. Sajab, C. H. Chia, C. H. Chan, S. Zakaria, H. Kaco *et al.*, *RSC Adv.*, **6**, 19819 (2016), <https://doi.org/10.1039/C5RA26193G>
- ⁸ S. Gan, S. Zakaria, R. S. Chen, C. H. Chia, F. N. M. Padzil *et al.*, *Mater. Chem. Phys.*, **192**, 181 (2017), <https://doi.org/10.1016/j.matchemphys.2017.01.012>
- ⁹ S. Gan, S. Zakaria, C. H. Chia and H. Kaco, *Cellulose*, **25**, 5099 (2018), <https://link.springer.com/article/10.1007/s10570-018-1946-5>
- ¹⁰ K. Baharin, S. Zakaria, A. Ellis, N. Talip, H. Kaco *et al.*, *Sains Malays.*, **47**, 377 (2018), <http://dx.doi.org/10.17576/jsm-2018-4702-20>
- ¹¹ S. Gan, S. Zakaria and S. N. S. Jaafar, *Carbohydr. Polym.*, **172**, 284 (2017), <https://doi.org/10.1016/j.carbpol.2017.05.056>
- ¹² K. M. Salleh, S. Zakaria, M. S. Sajab, S. Gan, C. H. Chia *et al.*, *Int. J. Biol. Macromol.*, **118**, 1422 (2018), <https://doi.org/10.1016/j.ijbiomac.2018.06.159>
- ¹³ X. Luo, X. Lei, N. Cai, X. Xie, Y. Xue *et al.*, *ACS Sustain. Chem. Eng.*, **4**, 3960 (2016), <https://doi.org/10.1021/acssuschemeng.6b00790>
- ¹⁴ H. Zhu, Y. Fu, R. Jiang, J. Yao, L. Xiao *et al.*, *Ind. Eng. Chem. Res.*, **53**, 4059 (2014), <https://doi.org/10.1021/ie4031677>
- ¹⁵ V. Rocher, J.-M. Siaugue, V. Cabuil and A. Bee, *Water Res.*, **42**, 1290 (2008), <https://doi.org/10.1016/j.watres.2007.09.024>
- ¹⁶ A. M. Muliwa, T. Y. Leswif, M. S. Onyango and A. Maity, *Sep. Purif. Technol.*, **158**, 250 (2016), <https://doi.org/10.1016/j.seppur.2015.12.021>
- ¹⁷ H. Fan, X. Ma, S. Zhou, J. Huang, Y. Liu *et al.*, *Carbohydr. Polym.*, **213**, 39 (2019), <https://doi.org/10.1016/j.carbpol.2019.02.067>
- ¹⁸ N. Barkoula, B. Alcock, N. Cabrera and T. Peijs, *Polym. Polym. Compos.*, **16**, 101 (2008), <https://doi.org/10.1177/02F096739110801600203>
- ¹⁹ X. F. Sun, B. Liu, Z. Jing and H. Wang, *Carbohydr. Polym.*, **118**, 16 (2015), <https://doi.org/10.1016/j.carbpol.2014.11.013>
- ²⁰ Z. Liu, H. Wang, C. Liu, Y. Jiang, G. Yu *et al.*, *Chem. Commun.*, **48**, 7350 (2012), <https://doi.org/10.1039/C2CC17795A>
- ²¹ I. Martín-Gullón and R. Font, *Water Res.*, **35**, 516 (2001), [https://doi.org/10.1016/S0043-1354\(00\)00262-1](https://doi.org/10.1016/S0043-1354(00)00262-1)
- ²² S. Babel and T. A. Kurniawan, *Chemosphere*, **54**, 951 (2004), <https://doi.org/10.1016/j.chemosphere.2003.10.001>
- ²³ N. A. Azahari, S. Zakaria, H. Kaco, S. Gan, C. H. Chia *et al.*, *Sains Malays.*, **46**, 795 (2017), <http://dx.doi.org/10.17576/jsm-2017-4605-14>

- ²⁴ S. Moosavi, S. Zakaria, C. H. Chia, S. Gan and N. A. Azahari, *Ceram. Int.*, **43**, 7889 (2017), <https://doi.org/10.1016/j.ceramint.2017.03.110>
- ²⁵ J. Qiu, L. Xu, J. Peng, M. Zhai, L. Zhao *et al.*, *Carbohydr. Polym.*, **70**, 236 (2007), <https://doi.org/10.1016/j.carbpol.2007.04.001>
- ²⁶ L. Ai, H. Huang, Z. Chen, X. Wei and J. Jiang, *Chem. Eng. J.*, **156**, 243 (2010), <https://doi.org/10.1016/j.cej.2009.08.028>
- ²⁷ C. S. Castro, M. C. Guerreiro, M. Gonçalves, L. C. Oliveira and A. S. Anastácio, *J. Hazard. Mater.*, **164**, 609 (2009), <https://doi.org/10.1016/j.jhazmat.2008.08.066>
- ²⁸ H. Y. Zhu, Y. Q. Fu, R. Jiang, J. Yao, L. Xiao *et al.*, *Bioresour. Technol.*, **105**, 24 (2012), <https://doi.org/10.1016/j.biortech.2011.11.057>
- ²⁹ Y. El-Shekeil, S. Sapuan, K. Abdan and E. Zainudin, *Mater. Des.*, **40**, 299 (2012), <https://doi.org/10.1016/j.matdes.2012.04.003>
- ³⁰ Y. Zhou, S. Fu, L. Zhang, H. Zhan and M. V. Levit, *Carbohydr. Polym.*, **101**, 75 (2014), <https://doi.org/10.1016/j.carbpol.2013.08.055>
- ³¹ X. Luo and L. Zhang, *J. Hazard. Mater.*, **171**, 340 (2009), <https://doi.org/10.1016/j.jhazmat.2009.06.009>
- ³² Y. S. Ho and G. McKay, *Process Saf. Environ. Prot.*, **76**, 183 (1998), <https://doi.org/10.1205/095758298529326>
- ³³ M. S. Sajab, C. H. Chia, S. Zakaria and P. S. Khiew, *Bioresour. Technol.*, **128**, 571 (2013), <https://doi.org/10.1016/j.biortech.2012.11.010>
- ³⁴ K. G. Bhattacharyya and A. Sharma, *J. Environ. Manag.*, **71**, 217 (2004), <https://doi.org/10.1016/j.jenvman.2004.03.002>
- ³⁵ D. H. K. Reddy and S.-M. Lee, *Adv. Colloid. Interface Sci.*, **201**, 68 (2013), <https://doi.org/10.1016/j.cis.2013.10.002>
- ³⁶ M. T. Yagub, T. K. Sen, S. Afroze and H. M. Ang, *Adv. Colloid. Interface Sci.*, **209**, 172 (2014), <https://doi.org/10.1016/j.cis.2014.04.002>
- ³⁷ S. Senthilkumaar, P. Kalaamani, K. Porkodi, P. Varadarajan and C. Subburaam, *Bioresour. Technol.*, **97**, 1618 (2006), <https://doi.org/10.1016/j.biortech.2005.08.001>
- ³⁸ I. S. A. Noor, Z. Sarani, S. Gan, C. H. Chia, C. Wang *et al.*, *Ind. Crop. Prod.*, **127**, 55 (2019), <https://doi.org/10.1016/j.indcrop.2018.09.056>
- ³⁹ H. Ansari, M. Miralinaghi and F. Azizinezhad, *Cellulose Chem. Technol.*, **53**, 191 (2019), [http://www.cellulosechemtechnol.ro/pdf/CCT1-2\(2019\)/p.191-204.pdf](http://www.cellulosechemtechnol.ro/pdf/CCT1-2(2019)/p.191-204.pdf)
- ⁴⁰ G. Biliuta, D. Suteu, T. Malutan, A.-I. Chirculescu, I. Nica *et al.*, *Cellulose Chem. Technol.*, **52**, 609 (2018), [http://www.cellulosechemtechnol.ro/pdf/CCT7-8\(2018\)/p.609-618.pdf](http://www.cellulosechemtechnol.ro/pdf/CCT7-8(2018)/p.609-618.pdf)